

EVALUATION OF THE J=0 FIXED POLE  
IN NEUTRON COMPTON SCATTERING

C. A. Dominguez, J. F. Gunion, R. Suaya  
Stanford Linear Accelerator Center  
Stanford University, Stanford, California 94305

ERRATA

1. In Eq. (6), p. 5, the last bracketed term should read

$$\left[ (p+q)^2 - (M+\mu_\pi)^2 \right]$$

2. In Eq. (10), p. 7, the first term should read

$$\sum_{n=0}^5$$

EVALUATION OF THE  $J=0$  FIXED POLE  
IN NEUTRON COMPTON SCATTERING\*

C. A. Dominguez†, J. F. Gunion, R. Suaya†  
Stanford Linear Accelerator Center  
Stanford University, Stanford, California 94305

ABSTRACT

We use the recent deuteron Compton data to evaluate the  $J=0$  fixed pole in neutron Compton scattering. This calculation includes the effects of both Glauber and Fermi motion corrections in the extraction of the free neutron cross section from the deuteron data. The result is consistent with the Born answer, zero. As a by-product, we show that the  $f:A_2$  ratio in Compton scattering is much larger than previously expected.

(Submitted to Phys. Rev.)

---

\*Work supported in part by the U. S. Atomic Energy Commission.

†Fellow of the University of Buenos Aires.

Recently there has been a great deal of speculation concerning the existence and nature of fixed poles in two photon processes. Damashek and Gilman, and also Dominguez, Ferro-Fontan, and Suaya,<sup>1</sup> have established that a description of the high energy data of on-shell proton Compton scattering requires, in addition to the standard Regge terms, a constant real part whose magnitude and sign agrees, within errors with the Thomson limit

$$f_1(0) = - \frac{\alpha}{M} . \quad (1)$$

It is tempting to interpret this extra real part as a "fixed pole" in the language of Reggeism. Many attempts have been made in the literature to understand the nature and source of such a fixed pole. In particular Brodsky, Close and Gunion<sup>2</sup> have shown that such a term arises naturally in any composite theory of the hadrons, when a pointlike coupling for the photon is allowed. Its residue has particularly simple behavior as a function of the photon mass squared in theories which exhibit exact scaling.<sup>3</sup> In such theories the fixed pole is seen as arising from the coherent sum of "seagull" terms for the individual proton constituents (quarks, bare hadrons). For the simplest composite systems (for which divergent Regge behavior is not present) the value of the fixed pole would be given by

$$- \sum_i \lambda_i^2 \alpha < \frac{1}{xM} > \quad (2)$$

where  $\lambda_i$  is the charge of the  $i$ th parton and  $x$  is the fraction of the incident hadron's momentum it carries in a properly chosen infinite momentum frame,<sup>2</sup>  $M$  is the hadron's total mass. Thus in the three quark model the ratio of the proton fixed pole to that of the neutron would be 3/2. Despite the fact that the prediction is no longer so simple in the presence of leading Regge behavior,

it is still true that the fixed pole probes the nature of the hadron's constituents in composite theories. In the most general case its value provides a constraint between the "wee" and the "hard" partons.<sup>4</sup>

This point of view is to be contrasted with that which relates the value of the fixed pole to the low energy theorem.<sup>5</sup> Were the fixed pole correlated with the Born term in this fashion then it should not occur in neutron Compton scattering. It would be most curious if a composite theory with scaling were to give a "Born" answer — that is if the sum of the bare constituent Born terms were to equal that of the composite particle.

In this paper we attempt to determine whether or not an additional constant real part is in fact required in the case of the neutron, using the recent results for Compton scattering on deuterium<sup>6</sup> and the available proton Compton data. In section I we discuss the calculable corrections to the deuterium data, their uncertainty, and possible modifications due to other more poorly understood deuteron effects. In section II we present the high energy Regge fits to the neutron total cross section necessary to an evaluation of the fixed pole. In section III we evaluate the relevant finite energy sum rules and obtain values for the fixed pole of the neutron as a function of the deuteron wave function and the high energy Regge parameters used. Surprisingly, the result is fairly independent of the deuteron wave functions, and except for extreme choices of the Regge parameters is consistent with zero. We have also calculated, for comparison, the value of the on-shell proton fixed pole. Our Regge parameters (determined using all available high energy data) differ somewhat from those used previously.<sup>1</sup> The value of the fixed pole is not, however, substantially altered.

## Section I

In this section we consider the corrections that must be made in order to extract the necessary integrals of the free neutron cross section. There are a number of effects which we do not attempt to correct for. These include those that would arise from a proper relativistic treatment of the deuteron, final state interactions, and the creation of virtual excited states within the deuteron. The magnitude of such corrections is not well known though there exist a variety of arguments that suggest they are small.<sup>7</sup> We shall, in what follows, ignore them.

We have attempted to include the Glauber corrections due to shadowing of one nucleon by the other and the "smearing" corrections considered recently by G. West and others.<sup>7</sup>

The Glauber corrections have been performed in the manner described by Hesse.<sup>8</sup> He gives the results for two extreme choices of the wave function of the deuteron, simple Gaussian and Gartenhaus, and for three possible choices of the ratio  $\frac{\text{Re}f}{\text{Im}f}$  for  $\gamma p \rightarrow \rho p$  in the forward direction. The Glauber corrections that we quote correspond to the mean of the above possibilities with errors which include both the uncertainty in  $\gamma p \rightarrow \rho p$  (forward) and the uncertainty due to wave function choice. Table 1 lists the Glauber correction as a function of energy, for  $\nu \geq 2$  GeV.

We consider in somewhat more detail the corrections due to Fermi motion as these are perhaps not as familiar as the Glauber ones. The effect arises because the energy of the photon-single nucleon collision varies according to the motion of the nucleons inside the deuteron. As a result the deuteron cross section (spin averaged) is given by

$$\sigma_D(\nu) = \int d^3\vec{p} \frac{\nu'}{\nu} \left[ f_S^2(|\vec{p}|) + f_D^2(|\vec{p}|) \right] \left[ \sigma_n(\nu', p^2) + \sigma_p(\nu', p^2) \right] \theta \left[ (p+q)^2 - (M+\mu_\pi)^2 \right] \quad (3)$$

where  $f_S(|\vec{p}|)$  and  $f_D(|\vec{p}|)$  represent the S and D wave components of the deuteron wave function and the invariants  $\nu'$  (the energy of the photon nucleon collision) and  $\nu$  (the total energy of the photon) are given by

$$\nu' = \frac{\vec{p} \cdot \vec{q}}{M}, \quad \nu = \frac{\vec{P} \cdot \vec{q}}{M_D} \quad (4)$$

$p$  and  $P$  are defined in Fig. 1 and are the nucleon and deuteron momenta respectively,  $M$  and  $M_D$  are their masses. The above equation, Eq. (3), is written in the incoherent single scattering approximation. In addition we shall neglect off-shell dependences of the single nucleon cross sections. We use the standard nonrelativistic normalization of the wave functions<sup>9</sup>

$$\int d^3\vec{p} |f(\vec{p})|^2 = 1 \quad (5)$$

Using Eq. (4) we rewrite Eq. (3) as

$$\sigma_D(\nu) = \frac{2\pi M}{\nu} \int_0^\infty \left[ f_S^2(|\vec{p}|) + f_D^2(|\vec{p}|) \right] |\vec{p}| d|\vec{p}| \int_{\nu'_-}^{\nu'_+} \nu' \sigma(\nu') d\nu' \theta \left[ (\vec{p} + \vec{q})^2 - (M + \mu_\pi)^2 \right] \quad (6)$$

where  $M\nu'_\pm = p^0 \nu \pm |\vec{p}| \nu$ . As suggested by West<sup>7</sup> we use four momentum conservation at the N-P-D vertex as for a Feynman graph.<sup>10</sup> In addition we note that in the single scattering approach the spectator nucleon is on-shell so that

$$p^0 = M_D - \sqrt{\vec{p}^2 + M^2} \quad (7)$$

To develop a bit of intuition concerning Eq. (3) we discuss the corrections at high energy where Regge theory presumably applies for the cross sections. Were we to neglect the  $\theta$  function of Eq. (3) then the effect of the screening corrections would be very small so long as the cross section is smoothly behaved. For instance, were the cross section constant for large  $\nu$  then

Eq. (3) without the  $\theta$  function would yield

$$\sigma_D(\nu) = \sigma \left\langle \frac{\nu'}{\nu} \right\rangle \quad (8)$$

From Eq. (4) we have

$$\left\langle \frac{\nu'}{\nu} \right\rangle = 1 - \frac{\epsilon + \langle T \rangle}{M} \quad (9)$$

where  $\epsilon$  = the binding energy of the deuteron and  $T$  is the relativistic kinetic energy of the spectator nucleon. The correction would then be below the 1% level. However, when the  $\theta$  function is present it limits the available phase space. For  $\nu \gg p^2, M^2$  it reduces to the requirement,  $\cos\theta < p^0/|\vec{p}|$ .

Which is restrictive if  $p^0$  of Eq. (7) is  $< |\vec{p}|$ . This phase space effect reduces the deuteron cross section relative to the sum of the neutron and proton cross sections. The magnitude of the correction will depend on the wave function used and is most sensitive to its high momentum components. That is it probes the short distance behavior of the wave function. It is thus clear that there is bound to be some change in the correction between "hard core" models and more smoothly behaved ones.

We have computed the above screening corrections for a variety of the most "accepted" deuteron wave functions (e.g., Hamada-Johnston, Lomon-Feshbach, Reid, Gartenhaus, etc.<sup>11</sup>) we consider the high energy region ( $\nu > 2$  GeV) and the low energy region separately.

The "unsmearing" of the low energy neutron cross section is in general a rather complicated business. One must first take the low energy proton cross section, correct it for Fermi motion, and subtract it from the deuteron experimental data to obtain the "smeared" (denoted in general by a superscript s) neutron data. (Glauber corrections are also necessary for  $\nu > 1.1$  GeV.) To obtain the

"unsmearred" neutron total cross section it is in general necessary to use an iterative procedure<sup>12</sup> in which one applies Eq. (3) to "test" neutron data to see if the output agrees with the smeared cross section calculated as above. However, in section III we shall see that we require only the low energy integral of the unsmearred neutron cross section. Using the proton data we find that an integral over the same low energy range of the smeared proton total cross section is related to the integral of the free proton cross section by a factor  $1 - \beta_{\text{eff}}$  which is nearly independent of the deuteron wave function. One can check that altering the proton data somewhat, performing the smearing and repeating the comparison of the smeared cross section integral to the unsmearred cross section integral, does not change the value of  $\beta_{\text{eff}}$ . Since the neutron cross section is quite similar in shape to the proton cross section, to a very good approximation one may calculate the integral of the unsmearred neutron cross section by dividing the smeared cross section by  $1 - \beta_{\text{eff}}$  as calculated using the proton data. (The deuteron wave function seen by the neutron is identical to that seen by the proton.)

The proton data used in the above procedure was taken from the Daresbury experiment for  $\nu > .265$  GeV. Below this we used extrapolated SLAC data, and the results of the Walker analysis of single pion photoproduction.<sup>6</sup> In order to compute the smeared proton cross section we used smooth fits to the free proton total cross section which incorporated five resonances plus a background of the form

$$\sum_{n=0}^S a_n (W - W_{\text{th}})^{n+1/2} \quad (10)$$

We use the parameterization of the first resonance region,  $P_{33}$ , given by Walker.<sup>13</sup> The 2nd, 3rd, 4th and "5th" resonances were parameterized using



standard nonrelativistic Breit-Wigner forms. The masses and widths of the resonances that result from the fits are close to the expected values if we attribute them to the  $P_{33}(1238)$ ,  $D_{13}(1520)$ ,  $F_{15}(1688)$  and  $P_{13}(1910)$ . The 5th resonance which we might identify as the Roper resonance was fixed at a 1.430 GeV. The  $\chi^2$  for the fit up to  $W$  (=cm energy) = 2 GeV is 35.3 for 71 degrees of freedom. The interpolating fit is shown in Fig. 2. (We remark here that the low energy integral,  $\int_{th}^2 \sigma_p(\nu) d\nu$ , which we use for the proton fixed pole calculation later, is some  $18\mu\text{b GeV}$  less than that calculated using extrapolated SLAC data only.)

The result of applying the Fermi motion correction to this proton input is shown in Figs. 2 and 3 for the Hamada-Johnston and Lomon-Feshbach (hard core) deuteron wave functions.  $\beta_{\text{eff}}$  as defined by

$$\int_{th}^N \sigma_p^S(\nu) d\nu = (1 - \beta_{\text{eff}}) \int_{th}^N \sigma_p(\nu) d\nu \quad (11)$$

where  $N$  is the cutoff point, is given in Table 2 for two cutoff choices and for a variety of wavefunctions. We then computed the smeared neutron cross section using

$$\sigma_n^S(\nu) = \sigma_D(\nu) - \sigma_p^S(\nu) + \sigma_G \quad (12)$$

The Glauber correction is zero below  $\nu = 1.1$  GeV.<sup>14</sup>

The resulting smeared neutron cross section is given in Figs. 3 and 4 for the Hamada-Johnston and Lomon-Feshbach hard core wave functions. We cannot resist making a comment concerning the appearance of the smeared cross section obtained above, namely that there appears to be a lack of any structure in the 3rd resonance region.<sup>15</sup>

Finally we calculated the integral of the free neutron total cross section as

$$\int \sigma_n(\nu) d\nu = (1 - \beta_{\text{eff}})^{-1} \int \sigma_n^{\text{S}}(\nu) d\nu \quad (13)$$

The values for this integral are tabulated in Table 2 for the various wave functions used. In calculating the above integral it was necessary to assume values for  $\sigma_n$  below  $\nu = 0.265$  GeV as there is no deuteron data below this value. In this region we simply assumed that the proton and neutron cross sections are the same as would be expected on the basis of the known isospin for the  $P_{33}$  resonance.

We consider in somewhat less detail the procedure followed for unsmearing the neutron data in the high energy region. There we require the smearing correction to each individual point as we wish in the end to make a Regge fit to the high energy data above  $\nu = 2$  GeV.

We first fitted the existing free proton total cross section data above  $\nu = 2$  GeV. We inserted this smooth interpolation of the high energy proton data into the smearing formula Eq. (3) and obtained a smeared version of the interpolating curve. By comparing this with the input curve we calculated

$$1 - \beta(\nu) = \frac{\sigma^{\text{S}}(\nu)}{\sigma(\nu)} \quad (14)$$

$\beta(\nu)$  as calculated above is fairly wave function dependent. We have presented the results for a variety of wave functions in Fig. 5. Typically it is of the order  $1.3 \times 10^{-2} \pm 25\%$ . It varies quite slowly with energy. One can also check that  $\beta$  is actually relatively independent of the high energy data used so long as no resonant structure is present and the general shape of the data is the same. This means that we may use this same  $\beta$  in unsmearing the neutron

data. In particular we calculated the free or unsmeared neutron cross section as

$$\sigma_n = \frac{\sigma_D}{1-\beta} - \sigma_p + \sigma_G \quad (15)$$

The error for each point was calculated using the experimental errors in the deuteron and proton total cross sections and the theoretical errors in  $\beta$  and in the Glauber correction,  $\sigma_G$ . Typically the errors in this final unfolded high energy neutron cross section are of the order  $12\mu\text{b}$ . (The experimental deuteron cross section error is typically  $10\mu\text{b}$ . The error in  $\beta$ ,  $0.3 \times 10^{-2}$ , combined with a  $250\mu\text{b}$  deuteron cross section contributes a  $0.75\mu\text{b}$  error to  $\sigma_n$ , while the proton cross section has a typical error of  $5\mu\text{b}$  and the Glauber correction is uncertain by  $1\mu\text{b}$ . Thus the major source of error lies in the experimental uncertainties.)

The results for  $\sigma_n$  (free) are presented in Fig. 6, where for convenience we have binned together some of the low energy points.<sup>16</sup>

## Section II

The final preliminary to calculating the value of the fixed pole is the determination of the Regge parameters appropriate to the high energy free neutron total cross section. We have assumed the simplest Regge behavior

$$\sigma_{p,n}(\nu) = A_{p,n} + \frac{B_{p,n}}{\sqrt{\nu}} \quad (16)$$

Corresponding to the presence of a Pomeranchuk term and an  $f\text{-}A_2$  Regge trajectory term. The intercept of the  $f\text{-}A_2$  has been taken from hadron physics at  $\alpha(0) = .5$ .<sup>17</sup>

The results of fitting the parameters A and B in Eq. (16) are presented in Table 3 for a variety of cutoffs, and in Fig. 6 (where we plot the fit with the low energy cutoff at  $\nu = 2\text{ GeV}$ ). We have also given in Table 3 and in

Fig. 6 the comparable fits to all proton data. Notable is the fact that the  $f-A_2$  trajectory for the neutron is comparable to that for the proton, 48 vs 52, with a similarly small difference in the Pomernanchuk term,  $98.6\mu\text{b}$  vs  $102.6\mu\text{b}$ , respectively. (Theoretically, of course, the Pomeron should be the same for both processes. One can perform a simultaneous fit to both cross sections with this constraint. The resulting parameters for the 2 GeV cutoff, also given in Table 3, are  $A_p = A_n = 101.7$ ,  $B_p = 53.7$ ,  $B_n = 41.3$  corresponding to a remarkably small  $A_2/f$  ratio = .13.) This is to be compared with earlier parameterizations of the high energy neutron cross section which quoted much lower  $B_n$  values than the above (e. g. , 33, with a Pomeron of 100, for the UCSB<sup>6</sup> data after Glauber corrections only).

### Section III

We are now ready to use finite energy sum rules to obtain values for the fixed poles of both neutron and proton Compton scattering. The basic sum rule<sup>18</sup> can be written

$$\text{Fixed Pole} = f(0) - \frac{1}{2\pi^2} \left[ \int_{\nu_0}^N \sigma_n(\nu) d\nu - (N\beta_P + 2\sqrt{N}\beta_{f-A_2}) \right] \quad (17)$$

$$f_p(0) = -3.0\mu\text{b GeV} \quad f_n(0) = 0.0\mu\text{b GeV}$$

where for  $\nu > N$  we have assumed that the leading Regge parameterization is an accurate representation of the cross section involved. The integral in Eq. (17) has already been given in Table 2 for the usual variety of deuteron wave function choices. The necessary Regge parameters appeared in Table 3.

In Table 4 we have tabulated the value of the fixed pole in neutron Compton scattering as a function of Regge parameters used (which of course depend somewhat on the cutoff of the high energy fit) and of the wave function.

Reasonably one can say that

$$\text{Fixed pole (neutron)} = 0.0 \pm 1.5 \mu\text{b GeV} \quad (18)$$

In Table 5 we present typical values for the proton fixed pole computed using Eq. (17) above with the Regge parameters of the proton high energy fit given in Table 3. The values are consistent with the Born answer

$$\text{Fixed pole (proton)} = -3.0 \pm 0.8 \mu\text{b GeV} \quad (19)$$

The errors in the above numbers were obtained by examining the range of values for the fixed pole which appear in Tables 4 and 5. For the neutron the wave function causes an uncertainty of about  $.3 \mu\text{b GeV}$  on the fixed pole while the error in the Regge parameters contributes about  $.9 \mu\text{b GeV}$  (as calculated from Eq. (17) using the error matrices resulting from the fitting program). The additional  $.3 \mu\text{b GeV}$  is designed to take into account the error in  $\ln$  resulting from altering the interpolation of the low energy data for the deuteron and proton. The error in the proton fixed pole includes  $.5 \mu\text{b GeV}$  from Regge uncertainties and  $.3 \mu\text{b GeV}$  from the low energy interpolation.

### Conclusion

We have shown that, using the new Daresbury data for deuteron Compton scattering, one obtains a result for the neutron fixed pole which is consistent with the Thomson limit (zero) as was the case in proton Compton scattering.

This presents interesting theoretical problems. The deep inelastic data appears to require a composite theory of the hadrons in which the photon interacts with the charged constituents. Nonetheless, the fixed pole seems to be sensitive only to the total charge, i. e., the noncomposite Born term, of the hadron.

## Acknowledgments

We want to express our gratitude to G. B. West and W. Atwood for providing us with the programs used to compute the smeared cross sections, and also R. Early for advise in the computation.

One of us (R.S.) acknowledges fruitful conversations with F. Gilman and S. Brodsky.

We thank C. Ferro Fontan for helpful correspondence.

Finally, two of us (C.A.D. and R.S.) would like to thank Prof. S. D. Drell for his kind hospitality at SLAC.

### Footnotes and References

1. M. Damashek and F. J. Gilman, Phys. Rev. D1, 1319 (1970); C. A. Dominguez, C. Ferro Fontan and R. Suaya, Phys. Letters 31B, 365 (1970); M. J. Creutz, S. D. Drell and E. A. Paschos, Phys. Rev. 178, 2300 (1969), originally suggested this possibility.
2. S. J. Brodsky, F. E. Close and J. F. Gunion, Phys. Rev. D (to be published), SLAC-PUB-973 and 1012.
3. Specifically its residue in the above mentioned theory is a simple polynomial in the photon mass. There exist a variety of theories for which this is not the case (e.g., the fixed pole residue in  $\frac{\nu T_2}{q^2}(\nu, q^2)$  could change sign as  $q^2$  goes negative). The on-shell value of the fixed pole, combined with a theory for its residue behavior, provides important constraints upon the neutron electroproduction data. The constraints in the simplest polynomial case have been discussed by F. E. Close and J. F. Gunion, Phys. Rev. D4, 742 and 1576 (1970). M. Elitzur, Phys. Rev. D3, 2166 (1971) and Y. Matsumoto, et al., Phys. Letters 39B, 258 (1972), have discussed the possibilities when the fixed pole is assumed to behave otherwise.

The neutron-proton mass difference when calculated using the Cottingham formula also requires knowledge of the same two pieces of input.

4. "Wee" partons are those which have a vanishingly small  $x$ , "hard" partons those which have a finite value of  $x$ .
5. H. Harari, in Proceedings of the Eleventh Session of the Scottish Universities Summer School in Physics 1970 (J. Cumming and H. Osborn, Eds.) Academic Press (New York, 1971).

6. T. A. Armstrong, et al., Daresbury preprint DNPL/P 105 (March 1972); H. Meyer, et al., Physics Letters B33, 189 (1970); D. O. Caldwell, et al., Phys. Rev. Letters 23, 1256 (1969); id 25, 609 (1970); W. P. Hesse, Thesis, University of California, Santa Barbara (1971) (unpublished); T. A. Armstrong, et al., Daresbury preprint DNPL/P 88 (October 1971); E. D. Bloom, et al., SLAC-PUB-653 (1969); J. Ballam, et al., Phys. Rev. Letters 23, 498 (1969), id. 21, 1544 (1968); H. G. Hilpert, et al., Phys. Letters 27B, 474 (1968); M. L. Perl, et al., Phys. Rev. Letters 23, 1191 (1969); J. T. Beale, S. D. Ecklund and R. L. Walker, California Institute of Technology Report CTSL-42 (1966).
7. G. B. West, Phys. Letters 37B, 509 (1971) and Stanford University preprint ITP-397 (Dec. 1971). G. Fäldt and T. E. O. Ericson, Nucl. Phys. B8, 1 (1968) make a similar analysis. The main difference arises in the phase-space factor whose effect was first discussed by West.
8. W. P. Hesse, see Ref. 6; V. Franco and R. J. Glauber, Phys. Rev. 142, 1195 (1966); S. J. Brodsky and J. Pumplin, Phys. Rev. 182, 1794 (1969).
9. For a discussion of the effects of a nonrelativistic normalization in the context of a semirelativistic treatment see G. B. West, Ref. 7.

The difference between a choice of a relativistic normalization such as e.g. ,

$$\int |f(\vec{p})|^2 \frac{p^0}{p_S^0} d^3\vec{p} = 1$$

and that given by Eq. (5) is very small in comparison with the uncertainties in the wave function itself.



Both treatments are equivalent provided that one identifies

$$f(\vec{p}) \left( \frac{M}{p_S} \right)^{1/2}$$

as the nonrelativistic wave function of the deuteron.

10. In a purely nonrelativistic approach this condition should be relaxed and the wave function should contain the relevant energy denominators. This and other possibilities are considered by A. Hacinliyan, *Nuovo Cimento* 8A, 541 (1972). Nevertheless the modification on our results is very small in the relevant region.
11. T. Hamada and I. D. Johnston, *Nucl. Phys.* 34, 382 (1962); R. V. Reid, *Ann. Phys. (N. Y.)* 50, 411 (1968); E. L. Lomon and H. Feshbach, *Ann. Phys. (N. Y.)* 48, 94 (1968); S. Gartenhaus, *Phys. Rev.* 100, 900 (1955); M. J. Moravcsik, *Nucl. Phys.* 7, 113 (1958).
12. R. L. Cool, *et al.*, *Phys. Rev.* D1, 1887 (1970). They did not include, however, the phase space constraint.
13. R. L. Walker, *Phys. Rev.* 182, 1729 (1969).
14. In principle one should take into consideration the effect of Fermi motion in reevaluating the Glauber correction at high energies. This modification is relatively small, however. Its main effect is to make the Glauber correction more independent of energy.
15. T. A. Armstrong, *et al.*, Ref. 6, also noticed this for their neutron cross sections. This lack of structure is to be expected in the quark model if the 3rd resonance region is dominated by the  $F_{15}(1688)$  (which is produced with  $\lambda = 3/2$  off protons). See Walker, Ref. 13 and R. P. Feynman, M. Kislinger, F. Ravendal, *Phys. Rev.* D3, 2706 (1971).

16. The Regge fits we discuss later were done without the binning.
17. Recently a variety of authors have noted, correctly, that changing the assumed  $f-A_2$  intercept results in a change in the value of the fixed pole provided the modification is fairly substantial. (The quality of the high-energy fit is not appreciably altered in the process.) However the  $f-A_2$  intercept is very well determined from purely hadronic processes to be  $0.5 \pm 0.1$ .
18. We have also used  $(1 - \beta_{\text{eff}})^{-1} \sigma_n^S(\nu)$  in the low energy region as input to a dispersion integral which calculates the real part of  $f_1(\nu)$  on the fashion of Damashek and Gilman, Ref. 1. Comparison of Ref., so calculated, with the Regge expression at high energy yields fixed pole values almost identical to those obtained from Eq. (17).

TABLE 1  
Glauber Corrections

$\nu$ (GeV)	$\sigma_G$ ( $\mu\text{b}$ )
2.0	2.3 $\pm$ 0.5
2.5	3.1 $\pm$ 0.6
3.0	3.5 $\pm$ 0.7
3.5	3.8 $\pm$ 0.8
4.0	4.0 $\pm$ 0.8
4.5	4.1 $\pm$ 0.8
5.0	4.2 $\pm$ 0.8
5.5	4.2 $\pm$ 0.8
6.0	4.3 $\pm$ 0.9
6.5	4.3 $\pm$ 0.9
7.0	4.3 $\pm$ 0.9
8.0	4.4 $\pm$ 0.9
9.0	4.4 $\pm$ 0.9
10.0	4.4 $\pm$ 0.9
11.0	4.4 $\pm$ 0.9
12.0	4.4 $\pm$ 0.9
13.0	4.4 $\pm$ 0.9
14.0	4.4 $\pm$ 0.9
15.0	4.4 $\pm$ 0.9
16.0	4.4 $\pm$ 0.9
17.0	4.4 $\pm$ 0.9
18.0	4.4 $\pm$ 0.9

TABLE 2  
 Integrals of the Free Neutron Cross Section  
 and  $\beta_{\text{eff}}$  for  $N = 2$  GeV.

Wave Function	$\beta_{\text{eff}}$	$I_n$ ( $\mu\text{b GeV}$ )
Hamada-Johnston (Hard Core)	0.022	335.9
Reid (Soft Core)	0.019	332.9
Lomon-Feshbach 1 (Hard Core)	0.028	339.6
Lomon-Feshbach 2* (Hard Core)	0.025	337.9

\* The two Lomon-Feshbach wave functions differ in the predicted amount of D-wave mixture (see Ref. 11).

TABLE 3

Regge Fits

 $\sigma_T(\gamma n)$ 

Fit No.	Cutoff GeV	$A_n$ ( $\mu\text{b}$ )	$B_n$ ( $\mu\text{b GeV}^{1/2}$ )	$\chi^2$	No. of points	Comments
1	2	98.6 $\pm$ 3.7	48.2 $\pm$ 8.4	99	140	with West corrections
2	2	95.7 $\pm$ 3.7	47.6 $\pm$ 8.4	97	140	without the West corrections
3	2	101.7 $\pm$ 1.7	41.3 $\pm$ 4.5	184	288	simultaneous fit to $\sigma_T(\gamma n)$ and $\sigma_T(\gamma p)$ with $A_n = A_p$
4	3	99.5 $\pm$ 4.6	45.1 $\pm$ 11.5	80	96	with West corrections
5	4	105.0 $\pm$ 6.0	28.1 $\pm$ 17.2	57.4	51	with West corrections
$\sigma_T(\gamma p)$						
		$A_p$	$B_p$			
1	2	102.6 $\pm$ 2.0	51.8 $\pm$ 4.3	84.6	148	includes all data
2	2	102.3 $\pm$ 2.0	53.0 $\pm$ 4.3	79	140	Without the data of Ballam, <u>et al.</u> , Hilpert, <u>et al.</u> , and Perl <u>et al.</u> , (Ref. 6).
3	2	101.7 $\pm$ 1.7	53.7 $\pm$ 3.8	184	288	Simultaneous fit to $\sigma_T(\gamma n)$ and $\sigma_T(\gamma p)$ with $A_n = A_p$ (all data)
4	3	104.2 $\pm$ 2.5	47.5 $\pm$ 6.0	65.8	101	includes all data
5	4	101.6 $\pm$ 3.3	55.4 $\pm$ 9.0	41.2	55	includes all data

TABLE 4  
Neutron Fixed Pole

Wave Function*	Fit No.	Fixed Pole ( $\mu\text{b} - \text{GeV}$ )	Error due to Regge parameter uncertainty
Hamada-Johnston (Hard Core)	1	-0.3	$\pm 0.9$
	2	-0.6	$\pm 0.9$
	3	-0.9	$\pm 0.5$
	4	-0.6	
Reid (Soft Core)	1	-0.0	$\pm 0.9$
Lomon-Feshbach 2 (Hard Core)	1	-0.3	$\pm 0.9$

\* Wave functions not given yield intermediate results.

TABLE 5

## Proton Fixed Pole

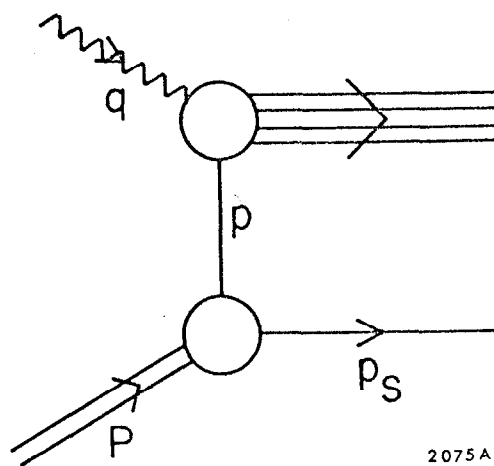
Fit No.	Fixed Pole ( $\mu\text{b-GeV}$ )	Error due to Regge parameter uncertainty
1	-3.7	$\pm 0.5$
2	-3.5	$\pm 0.5$
3	-3.4	$\pm 0.4$
4	-3.1	$\pm 0.6$

## Figure Captions

1. Kinematics.
2. Experimental points of  $\sigma_T(\gamma p)$  (open circles) and smeared photon-proton total cross sections,  $\sigma_T^S(\gamma p)$  (x) using the Hamada-Johnston wave function. The continuous curve is the result of our fit to the experimental points.
3. Smeared  $\sigma_T^S(\gamma p)$  (closed circles) and  $\sigma_T^S(\gamma n)$  (open circles) using the Hamada-Johnston wave function. (Below  $\nu = 0.265$  GeV we use  $\sigma_T^S(\gamma n) = \sigma_T^S(\gamma p)$ .)
4. Smeared  $\sigma_T^S(\gamma p)$  (closed circles) and  $\sigma_T^S(\gamma n)$  (open circles) using the Lomon-Feshbach wave function. (Below  $\nu = 0.265$  GeV we use  $\sigma_T^S(\gamma n) = \sigma_T^S(\gamma p)$ .)
5.  $\beta$  as a function of photon energy,  $\nu$ , for the following wave functions:
  1. Lomon-Feshbach 1 (Hard Core)
  2. Lomon-Feshbach 2 (Hard Core)
  3. Reid (Hard Core)
  4. Hamada-Johnston (Hard Core)
  5. Reid (Soft Core).
6. High energy photon-neutron total cross sections
  - ◻ Binned Daresbury data
  - UCSB (Ref. 6)
  - DESY (Ref. 6).

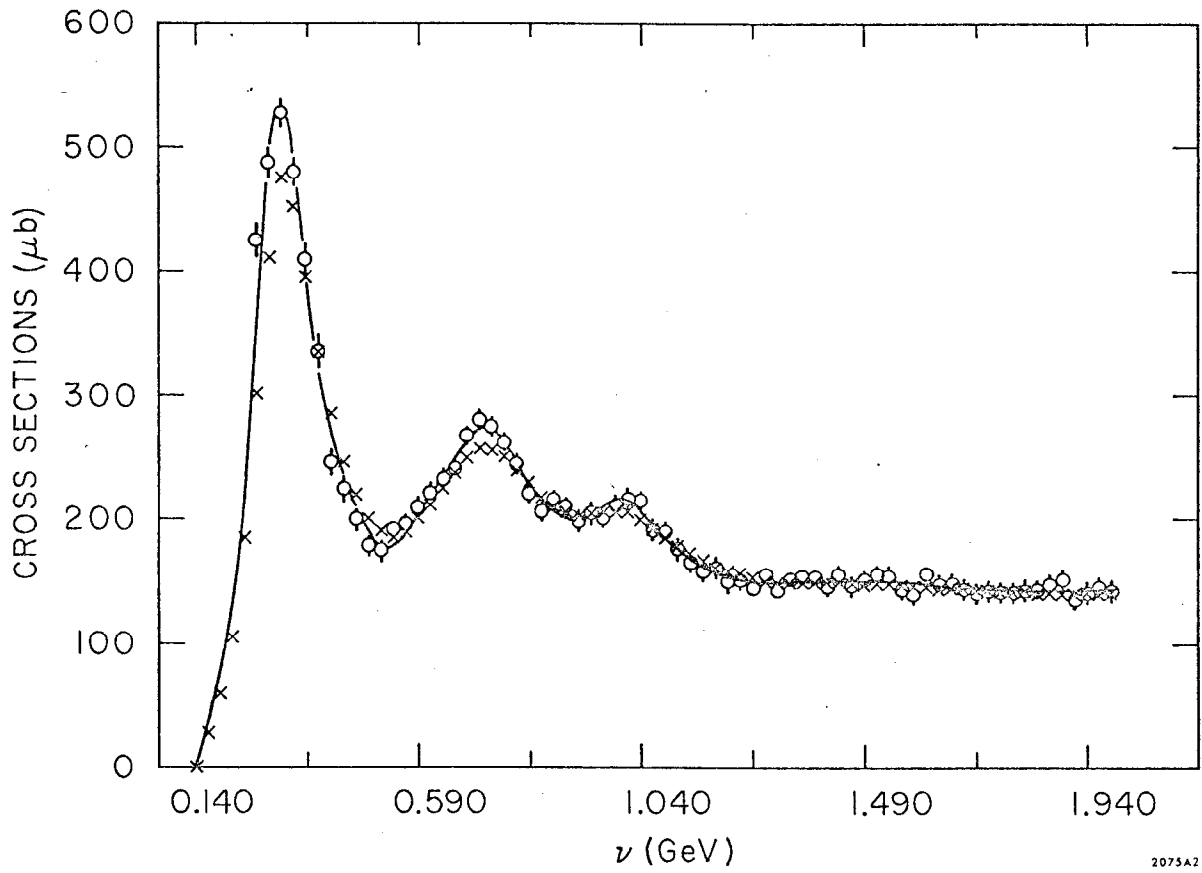
The neutron Regge fit corresponds to fit 1. Fit to  $\sigma_T(\gamma p)$  is drawn for comparison (see Table 3).





2075 A7

Fig. 1



2075A2

Fig. 2

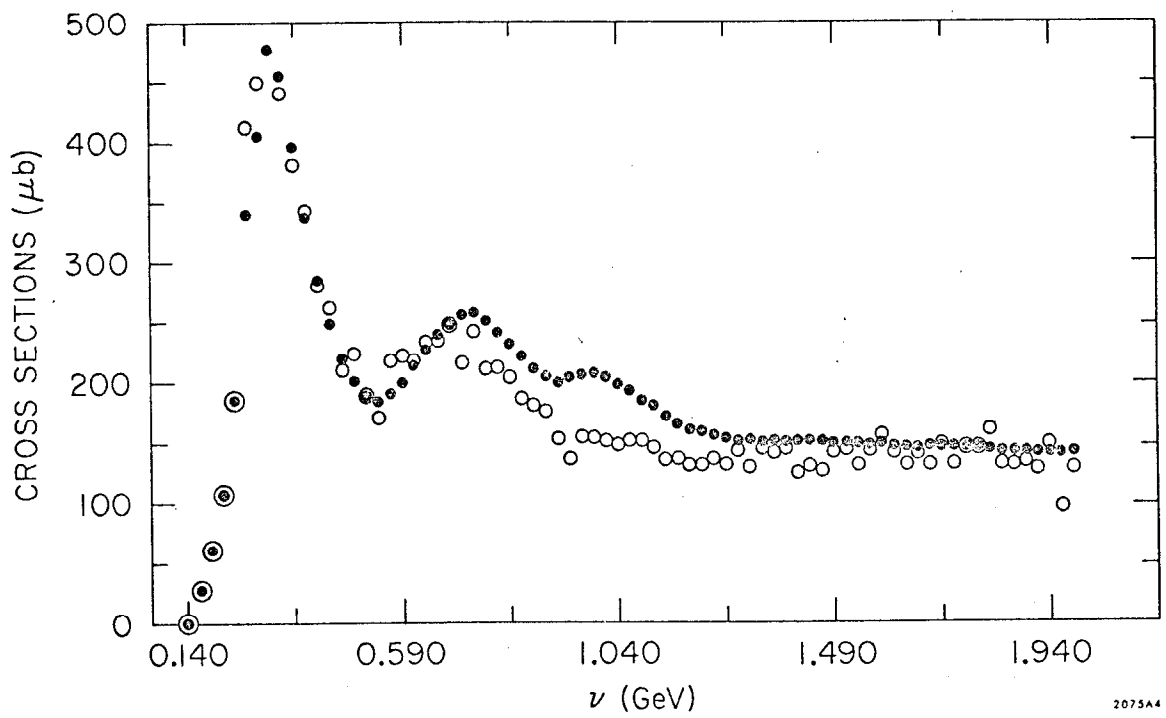
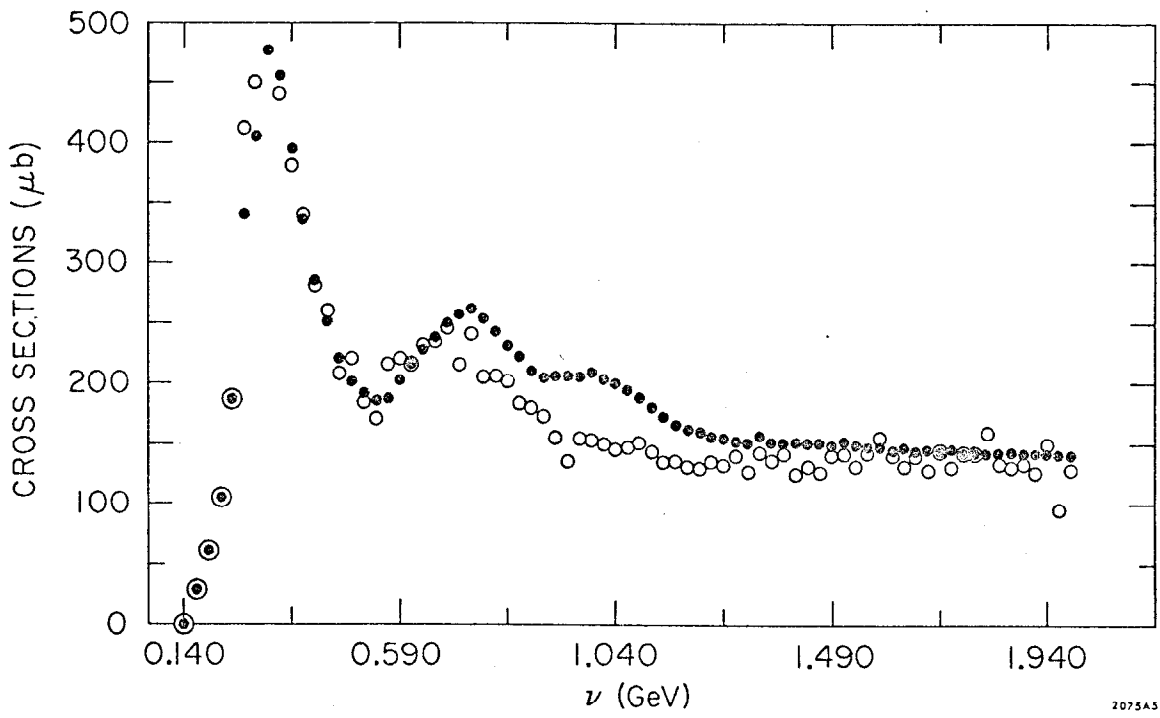
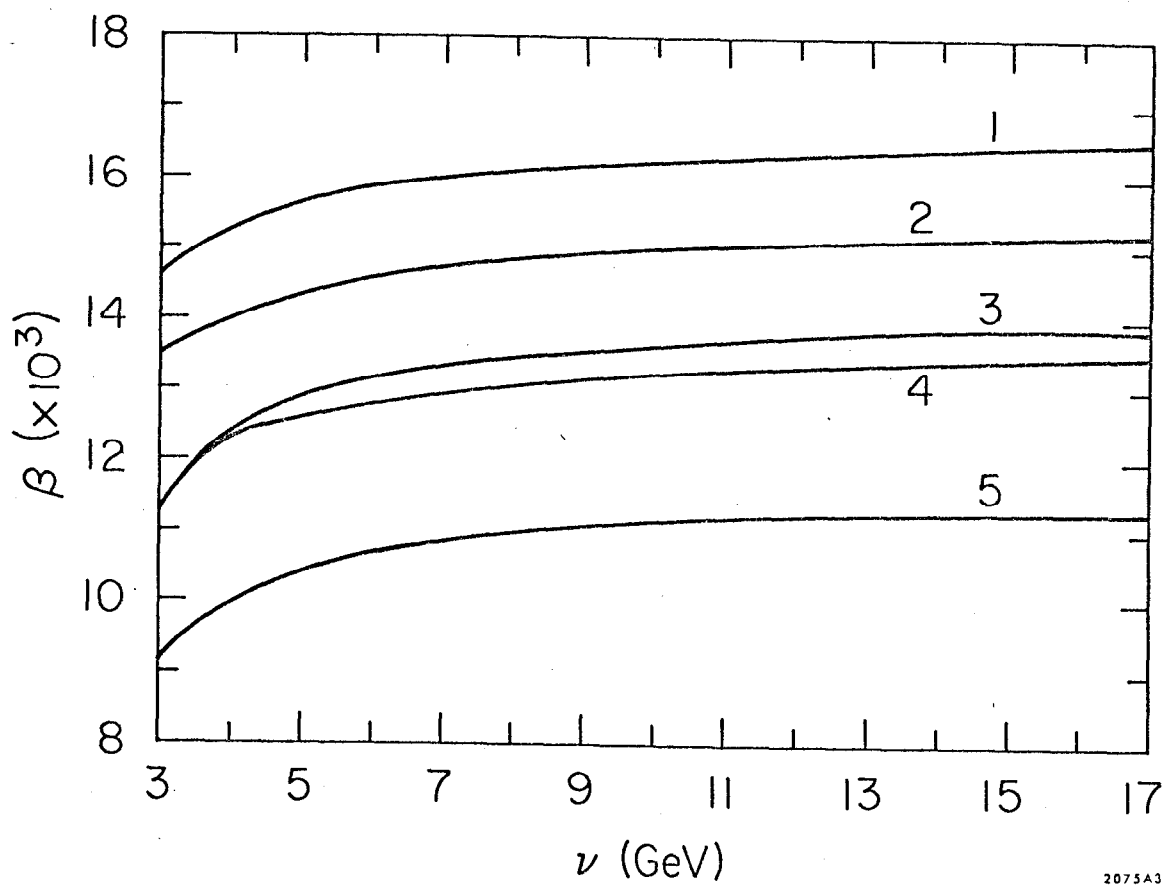


Fig. 3



2075A3

Fig. 4



2075A3

Fig. 5

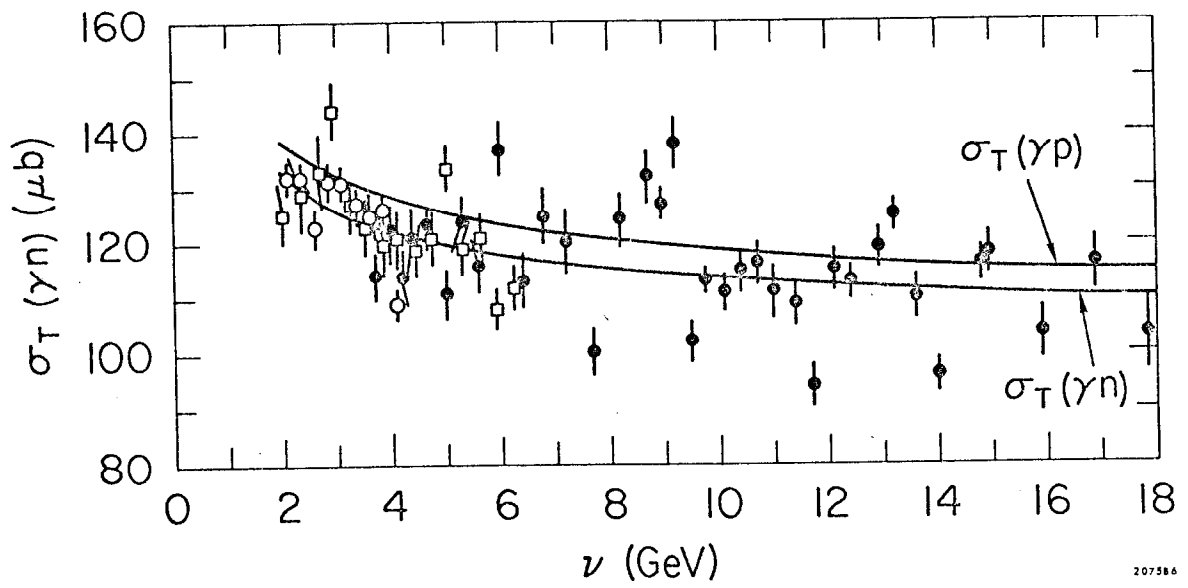


Fig. 6